

MAGMA – Multimodal Augmentation of Generative Models through Adapter-based Finetuning

Constantin Eichenberg*, Sidney Black*, Samuel Weinbach

Aleph Alpha

sdtblck@gmail.com

{constantin.eichenberg, samuel.weinbach}@aleph-alpha.de

Letitia Parcalabescu, Anette Frank

Heidelberg University

{frank, parcalabescu}@cl.uni-heidelberg.de

Abstract

Large-scale pretraining is fast becoming the norm in Vision-Language (VL) modeling. However, prevailing VL approaches are limited by the requirement for labeled data and the use of complex multi-step pretraining objectives. We present MAGMA - a simple method for augmenting generative language models with additional modalities using adapter-based finetuning. Building on Frozen [52], we train a series of VL models that autoregressively generate text from arbitrary combinations of visual and textual input. The pretraining is entirely end-to-end using a single language modeling objective, simplifying optimization compared to previous approaches. Importantly, the language model weights remain unchanged during training, allowing for transfer of encyclopedic knowledge and in-context learning abilities from language pretraining. MAGMA outperforms Frozen on open-ended generative tasks, achieving state of the art results on the OKVQA benchmark and competitive results on a range of other popular VL benchmarks, while pretraining on $\sim 0.2\%$ of the number of samples used to train SimVLM [55].

1. Introduction

Self-supervised representation learning with transformer models [53] has become the dominant technique in Natural Language Processing in recent years, with encoder transformer models trained using a Masked Language Modeling (MLM) objective [12] excelling at Natural Language Understanding tasks, and autoregressive decoder models [6, 38, 39] displaying impressive Natural Language Generation at increasingly large scales. Vision Language (VL)



Q: What caused the mess on the carpet? A:

The dog.

Q: What caused the mess on the carpet? A:

The carpet was stained by a spilled drink.

Figure 1. An example output produced by MAGMA. For this and all following examples the input text is displayed in black, and the model’s response in green.

modeling – the modeling of joint image-text representations for tasks such as image captioning or visual question answering – has followed suit, with the transformer encoder becoming the prevalent architecture in recent research. A popular approach among the latest state of the art VL models is to use a BERT-style encoder language model (LM) in combination with an object detection backbone such as Faster-RCNN [41]. This approach, while displaying impressive performance on challenging benchmarks, has a number of drawbacks (see Section 2), in particular not being able solve VL tasks in an open-ended, generative fashion.

A recent line of work [47, 52, 55] explores VL modeling using autoregressive decoder models trained with a language modeling objective. SimVLM [55], while showing impressive performance, requires a prohibitively large amount of data for pretraining and the language and vision components to be trained in tandem. Frozen [52] shows

*Equal contribution

that a pretrained autoregressive language model can, without any finetuning to the LM weights themselves, be harnessed to train a visual prefix which enables images to be used as its input. While the performance of *Frozen* on VL benchmarks falls short compared to the state of the art, we feel the approach is promising due to its practicality, and the public availability of large, pretrained LMs such as GPT-J [54], PanGu- α [59], and GPT-Neo [3].

Extending the *Frozen* approach, in this paper we introduce a framework to combine existing unimodal language and unimodal vision models pretrained on large web datasets into a powerful multimodal model. Specifically, our contributions are the following:

- We introduce MAGMA: An autoregressive VL model that is able to generate text from an arbitrary combination of visual and textual input. Like *Frozen*, we start from a fixed large LM and a visual encoder-prefix stack. MAGMA differs from *Frozen* by additionally augmenting the LM with adapter layers, and using CLIP’s [37] visual component as an encoder. Only training the adapters and visual components, the method is parameter efficient and naturally retains the LM’s encyclopedic knowledge and *in-context* learning abilities.
- Pretrained on a simple next token prediction objective, MAGMA is competitive in several VL downstream tasks, significantly outperforming its predecessor, *Frozen*, while pretraining on $\sim 0.2\%$ of the number of samples used to train *SimVLM* [55]. In particular, MAGMA achieves state of the art accuracy on the OKVQA benchmark, which we evaluate as a fully open-ended generative task.
- We run extensive ablations on the vision encoder and adapter components – showing that a pretrained CLIP ResNet encoder outperforms other visual backbones, that a model trained with adapters outperforms a visual prefix only method, and that different adapter configurations excel at different downstream tasks.
- We show that a carefully curated pretraining dataset, which includes around 25 million image-text pairs from a wide range of sources, including downstream task benchmarks, can dramatically increase zero shot performance when compared to a noisier, web-scraped dataset (CC12M [7]).

While we only explore the vision-language domain in this work, we expect the general method of a modality-specific prefix in combination with adapter layers and a frozen LM to apply equally well to other combinations of modalities, such as audio-text pairs.

In addition to this publication, we plan to open-source our trained model weights and code in the near future.

2. Related Work

The canonical approach [10, 28, 29, 50, 51, 60] to building VL models in the past few years generally harnesses a BERT-like encoder transformer model as the language component, trained with a MLM objective – where random words in the input are masked out, and the model is tasked with predicting them. Encoder VL models are often also pretrained with auxiliary objectives or custom cross-modal loss functions, such as the Masked Region Modeling, Image-Text Matching and Word-Region Alignment of UNITER [10], or the contrastive loss of OSCAR [29]. The use of auxiliary cross-modal loss functions and pretraining tasks complicates the pretraining procedure by requiring these losses to be properly balanced. Additionally, encoder models require an extra task-specific finetuning step for each task in order to perform effectively, limiting their accessibility. In comparison, autoregressive VL models like MAGMA are trained on a single, simple next token prediction objective, and can perform well on a wide range of tasks without any further finetuning.

Two direct predecessors to our method are *Frozen* [52] and *SimVLM* [55], two autoregressive decoder models trained with a next token prediction language modeling objective. *Frozen* affixes an NFResnet [5] vision encoder to a pretrained autoregressive LM and, keeping the LM weights frozen, trains the vision encoder along with a *visual prefix* that linearly maps the output of the vision encoder to the dimensionality of the LM’s token embeddings. *Frozen* shows that autoregressive VL models have the ability to adapt to examples *in-context*, like their language only counterparts [6], without performing any gradient updates. When shown multiple examples of a task in its context window in *Few-Shot learning*, its performance on that task improves, it appears to ‘learn’ from the presented examples without any task-specific finetuning. Our model has similar *in-context* learning capabilities, but the addition of adapters and the different choice of visual backbone results in a model with improved performance when trained on a comparable dataset, see Section 3.3.

SimVLM takes a similar approach to *Frozen*, but performs the pretraining of the vision and language components in tandem using a prefix LM objective. Their model consists of an encoder-decoder transformer with a combined ResNet [19] and ViT [13] backbone as encoder, and a transformer decoder for language modeling. *SimVLM* performs impressively, extending the state of the art on a wide range of benchmarks, and showing that a simple language modeling task can outperform MLM approaches. However, the joint pretraining requires prohibitively large uni- and multimodal datasets (1.8 Billion+ image-text pairs and ~ 800 GB of raw text), and long training times (~ 4 Billion image-text pairs and ~ 130 Billion text tokens). Aside from using orders of magnitude less data than *SimVLM*,

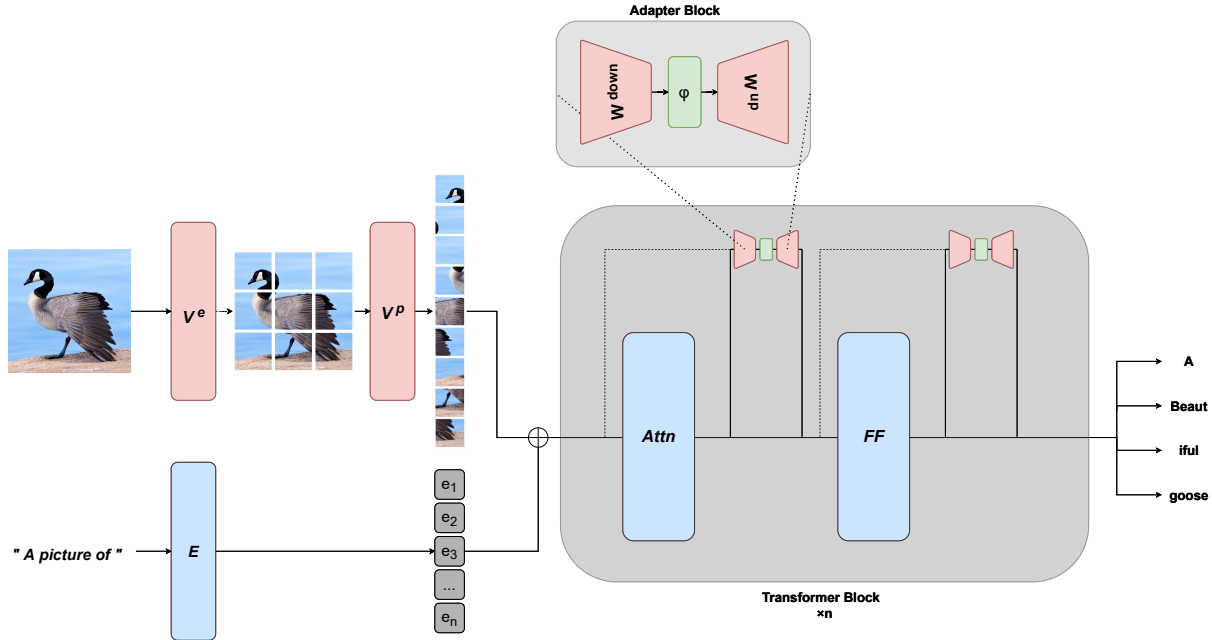


Figure 2. MAGMA’s architecture. The layers in red are trained, and the layers in blue remain frozen.

MAGMA allows for the full recovery of the underlying LM’s performance by simply removing the adapter layers.

Our work builds heavily on recent advances in parameter efficient finetuning of LMs [18, 20, 21, 27, 30]. Specifically through the use of adapter layers [18, 20, 34], small modules inserted in between the elements of a transformer layer which are finetuned instead of the model weights as a form of parameter efficient fine-tuning.

For a visual backbone, a common approach is to use region features extracted from a pretrained object detection model such as Faster-RCNN [41] as the visual input. Due to the use of region features, the classes of objects the resultant model can recognize is heavily limited, as object detection models are generally trained using expensive human labelled data on a bounded set of object classes. On the other hand, contrastive models such as CLIP [37] and ALIGN [24] present a more robust approach to learning visual features by learning joint representations between image-text pairs. This class of models show strong performance on a wide variety of vision tasks as well as impressive generalization abilities that can provide powerful semantic guidance to image generation [14], but since they were only trained to match image-text pairs, cannot inherently be used for tasks that require text generation as an output [44].

However, [44] show that the weights of contrastive language-image models contain useful semantic information for VL tasks. By replacing the conventional region-based backbone with CLIP’s visual encoder in popular VL

architectures, the authors achieve SOTA results across a wide variety of VL tasks without the need for region-based features, motivating us to use CLIP’s visual component as a vision encoder for MAGMA. Notably, we confirm their finding that the ViT variant of CLIP underperforms on VL tasks when compared to the ResNet variant, particularly in tasks that require localization within an image.

3. Method

Our general approach is an image conditioned variant of soft-prompting or prefix tuning [27, 36, 45] for language transformers and is an extension of the *Frozen* method introduced in [52]. The core concept is to translate image features into language embeddings carrying visual information which can therefore be interpreted by the language transformer without need to retrain the latter from scratch.

3.1. Architecture

The model can be broken down into four main components, see Figure 2. First, images are fed into a *Visual Encoder*, which processes the raw image input and outputs a sequence of feature vectors. Then an *Image Prefix* module maps the image features into a sequence of embedding vectors that are input to the third model component, an autoregressive *Language Model*. The fourth component is a series of *Adapter* layers which are inserted into the transformer LM, and tuned during training. Below we discuss the four components in more detail.

Visual Encoder - V^e . The visual encoder is a network used to extract condensed semantic information about an image. In principle, the visual encoder could take the form of any deep vision network whose output can be mapped to a sequence of embedding vectors. For our ablations, we use the visual backbone of several variants of CLIP. We also train a model with an NFResnet encoder trained from scratch, a variant analogous to the model presented in *Frozen*, see Section 4.2. The output of the visual encoder is then passed into the *Image Prefix*.

Image Prefix - V^p . Before the output of the encoder can be input to the LM, it needs to be translated into a sequence of n vectors of dimension d_h , where d_h is the hidden dimension of the LM. For the CLIP encoders, we extract the feature grid before the pooling layers, resulting in an $N \times N$ grid, where $N = 7, 7, 12$ for the 'ViT-B/32', 'RN50x4' and 'RN50x16' variants of CLIP respectively. We then flatten the feature grid into a sequence of N^2 vectors, and linearly transform the vectors' channel dimension to d_h . For the NFResnet variant, we follow the procedure described in *Frozen* by linearly transforming the output to $d_h \cdot n$, where n can be an arbitrary sequence length which we set to 2. Finally, we apply dropout regularization to the output of the image prefix, followed by Layer Normalization. We also explored non-linear variants of prefix mappings, replacing the linear transformation with an MLP and a transformer encoder, but found no improvements.

Language Model - E, T, H . The language backbone of our architecture is initialized from a pretrained autoregressive transformer LM similar to GPT [38].

A text input y is first converted into a sequence of tokens t_1, \dots, t_m . Then a word embedding layer E maps each token t_k to a unique vector $e_k = E(t_k) \in \mathbb{R}^{d_h}$, obtaining a sequence of embeddings e_1, \dots, e_m which are input to a transformer-decoder module T with a causal attention mask. A language model head H then maps the final output embeddings of the transformer to logits over the token space which can be used in a cross-entropy loss function for a next-token-prediction training objective and to autoregressively generate text during inference. The fact that any sequence of vectors $v_1, \dots, v_m \in \mathbb{R}^{d_h}$ can be used as input to the transformer enables us to use images as input after mapping them through the encoder and the prefix as described above.

For the LM component, we use the open sourced weights of the 6 Billion parameter LM, GPT-J [54]. Since GPT-J's architecture is largely similar to that described in [38], we will not cover it in this paper, but do note two key differences of GPT-J compared to the original GPT architecture. Firstly, GPT-J replaces learned positional embeddings with rotary positional embeddings [49], a form of relative po-

sitional embedding. As noted in [52], relative positional embeddings enable the transformer to generalize to inputs with more than one image, or a different image-text ordering compared to the training distribution, which is key to the VL model's ability to perform in-context learning with multiple image examples. Secondly, the attention layer and the feedforward layer are computed in parallel for decreased communication costs [54].

Adapters - $\{A_i\}$. Adapters are a series of small modules generally placed in between elements of a transformer model [20], that can be finetuned in place of the model weights as a form of parameter efficient fine-tuning. We use the framework of [18], where the adapter layers generally take the form of a scaled residual bottleneck MLP

$$A_i(h) = h + \lambda_i W_i^{up} \varphi(W_i^{down} h). \quad (1)$$

The matrices $W^{down} \in \mathbb{R}^{d_b \times d_h}$ and $W^{up} \in \mathbb{R}^{d_h \times d_b}$ with $d_b < d_h$ constitute the bottleneck, φ is an activation function (in our case ReLU) and λ_i is a scaling parameter that is either trained or set equal to 1. We refer to the ratio d_h/d_b as the **downsample factor** of the adapter.

Given a set of adapters $\{A_i\}$ and a transformer module T , we denote the adapted version of T by \tilde{T} , which means replacing the attention and/or feed-forward blocks B_i of T by their adapted version \tilde{B}_i , either obtained from adding the adapters in parallel or sequentially:

$$\tilde{B}_i: h \mapsto \begin{cases} B_i(h) + A_i(h) & (\text{parallel}) \\ B_i(h) + A_i(B_i(h)) & (\text{sequential}) \end{cases} \quad (1)$$

We run experiments with both the parallel and the sequential adapter variants, see Section 4.2.1 for results.

3.2. Training

During training, the weights of the LM E, T, H remain unchanged, whereas the weights of the image encoder, image prefix and the adapters are optimized. In the following we denote the trainable parameters of a module by the subscript θ . As described in 3.1, a set of trainable adapters $\{A_{i,\theta}\}$ gives rise to the modified transformer module \tilde{T}_θ .

The training objective is a captioning task: given an image-caption pair (x, y) , we embed the image as $v_{1,\theta}, \dots, v_{n,\theta} = V_\theta^p \circ V_\theta^e(x)$ and the text as $e_1, \dots, e_m = E(t_1), \dots, E(t_m)$, where $\{t_k\}$ is the tokenized caption y . Note that the image sequence length n is fixed while the length of the caption m is variable. The image embeddings are then prepended to the text embeddings and fed through the adapted transformer module. Denoting the embedding-to-logits function as $l_\theta = H \circ \tilde{T}_\theta$, we then compute the loss

$$L_\theta(x, y) = - \sum_{i=1}^m l_\theta(v_{1,\theta}, \dots, v_{n,\theta}, e_1, \dots, e_i), \quad (2)$$

where $l_\theta(v_{1,\theta}, \dots, v_{n,\theta}, e_1, \dots, e_i)$ is interpreted as next-token log-probability conditioned on the previous sequence elements

$$l_\theta(v_{1,\theta}, \dots, v_{n,\theta}, e_1, \dots, e_i) = \log p_\theta(t_i | x, t_1, \dots, t_{i-1}). \quad (3)$$

The above loss function highlights the similarity of our method to general prefix tuning, where the prefix in this case is given by the image embeddings.

3.3. Dataset

For all ablations in 4.2 we train on CC12M [7] for a total of around 3M samples ensuring comparability with *Frozen*. Unfortunately, CC12M performs hypernyming, replacing any names of people with $\langle \text{PERSON} \rangle$. This causes downstream models to output $\langle \text{PERSON} \rangle$ overwhelmingly often, even when the inputs do not contain people or places.

This failure mode, as well as recent research suggesting that increased training dataset diversity improves downstream generalization capabilities [6, 15, 37, 60], prompted us to construct a large-scale pretraining dataset from various publicly available image-text datasets, including a filtered version of LAION [43], Wikipedia Image-Text [48], CC3M [8], Visual Genome [26] and Localized Narratives [35].

Following research demonstrating that LMs become strong zero-shot learners after being finetuned on collections of structured, task-based datasets [42, 56], we also opt to include the training sets of various downstream tasks – adding the train sets of VQA [2], GQA [23], OKVQA [31], VizWiz [17], Hateful Memes [25], and CoCo Captions [9], resulting in a final dataset of around 25 million image-text pairs.

4. Experiments and Analysis

To evaluate the methodology laid out in the previous sections, we first train a series of ablations, 4.2, in order to break down the effects of the choice of vision encoder and adapter respectively. We evaluate these ablations, and all subsequent models, on a range of *visual question answering* and *image captioning* tasks designed to quantify the model’s ability to adapt to new tasks using *in-context* learning, recognize a wide variety of objects, and reason in detail about an image – often involving the use of complex spatial understanding, encyclopedic world knowledge, and optical character recognition (OCR).

During pretraining for the ablations and all subsequent models, we update the parameters θ by minimizing the loss (2) per mini-batch using the Adam optimizer in combination with *ZeRO* [40] to parallelize gradients and optimizer states across devices. We train all models with a batch size of 256, a dropout probability of 0.1, a weight decay of 0, and use learning rates of $2 \cdot 10^{-6}$ for V_θ^e and

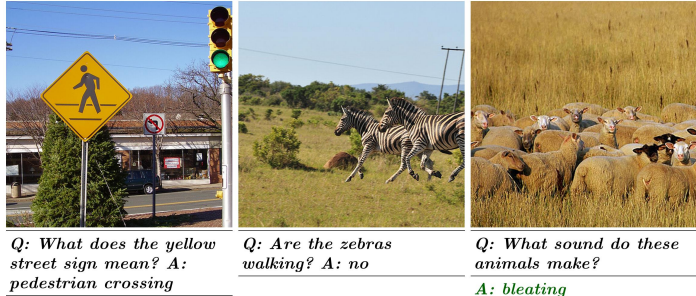


Figure 3. An example of a 2-shot prompt for OKVQA.

$8 \cdot 10^{-4}$ for $(V_\theta^p, \{A_{i,\theta}\})$, annealing both to 10% of their original value using a cosine decay schedule throughout training. When finetuning on downstream tasks (see Section 4.3) we do early stopping based on validation loss, and use the same hyperparameters as above, aside from decreasing the learning rates for V_θ^e , $(V_\theta^p, \{A_{i,\theta}\})$ to $1.5 \cdot 10^{-6}$, $7 \cdot 10^{-4}$ for generative tasks and $1.5 \cdot 10^{-6}$, $3 \cdot 10^{-4}$ for SNLI-VE classification. We also independently replicate the *Frozen* model, denoted MAGMA_{froz} , using the pre-training setup described in their paper (with the exception that we pretrain on CC12M) to use as a baseline. We build our model using the PyTorch framework with Deepspeed for data-parallel training – training all ablations on 32 A100 GPUs for around 1.25 days each.

4.1. Evaluations

4.1.1 Visual Question Answering

Visual Question Answering tasks require the model to respond to a question about the input image. Breaking from previous works, which generally formulate Visual Question Answering tasks as classification tasks over the most frequent responses in the training set, we formulate all Visual Question Answering tasks as open-ended generative tasks to enable few-shot prompting. We use the following datasets:

VQA 2.0 [2]. A large and commonly used dataset for visual question answering where each datapoint consists of an image, a question regarding the content of the image and 10 corresponding ground-truth answers.

OKVQA [31]. A QA dataset where all questions require explicit outside world knowledge not contained in the picture to be answered correctly.

GQA [23]. A large QA dataset with a heavy focus on visual and spatial reasoning, where a datapoint consists of an image, a question and one ground-truth answer.

VizWiz [17]. A dataset in the same format as VQA where the questions were asked by visually impaired people. The ground-truth to a question about an image may be “unanswerable” or “unsuitable”, which has to be recognized by the model.

To compare the generated model output with the provided ground-truths, we apply the normalization procedure described in the official VQA 2.0 repo¹, and truncate the model output to the length of the longest ground truth answer. In the case of VQA, OKVQA, and VizWiz, which all provide multiple ground truth answers, we calculate the accuracy metric as described in the official VQA paper [2], and for GQA we use the canonical accuracy score.

For few-shot settings, we use the procedure described in [52], simply prepending n random examples of completed tasks before each question answer pair. We prepend "Q: " and "A: " to each question and answer respectively, finding that this results in superior performance. See Figure 3 for an example.

4.1.2 Image Captioning

Image captioning tasks require the model to generate accurate descriptions of input images in natural language. We evaluate on two datasets – CoCo Captions [9] and NoCaps [1], measuring performance using the BLEU@4 and CIDEr metrics. NoCaps is designed to evaluate a model’s ability to caption images containing uncommon or novel object classes that don’t appear in CoCo.

Like *SimVLM*, we observe that prefixing “A picture of” to the image captioning prompt dramatically increases downstream scores – for $MAGMA_{long}$, increasing the CIDEr score on CoCo Captions from 7.5 to 57.1. All scores reported in Table 1 use this as a prefix. Other prefixes, such as “Caption:” have a similar effect.

4.1.3 Visual Entailment

We test Visual Entailment performance on SNLI-VE [57], a task built on top of SNLI [4]. SNLI-VE is a classification task that requires the model to reason about the relationship between an *image premise*, P_{image} , and a *text hypothesis*, H_{text} . Given P_{image} and H_{text} as model input, the task is to choose a label from a set of three labels - entailment, neutral and contradiction - that best describes the relationship between the two. We formulate SNLI-VE as a classification task by finetuning the model together with a linear classification head that takes as input the last-layer transformer embedding corresponding to the last text token.

4.2. Ablations

We run two series of ablations: one designed to test the impact of the adapter layers and their precise configuration, and another designed to test the impact of the vision encoder choice. All ablations are trained for a total of 15000 steps, or around 3.8 million image-text pairs.

¹<https://github.com/GT-Vision-Lab/VQA>

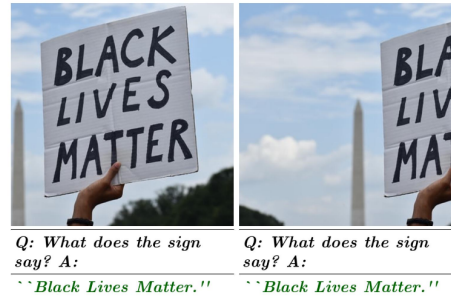


Figure 4. An example of MAGMA’s OCR capabilities. Note that, even when the text is obscured, MAGMA is able to impute the missing values.

4.2.1 Adapter Types

We run ablations with several different adapter configurations, motivated by [18] showing that the precise formulation of the adapter layer can have a large impact on the performance of a model on downstream tasks, as well as the fact that different adapter layers can perform better than others dependent on the task. Since an exhaustive sweep in the parameter space of adapters is very expensive, we decided on seven specific configurations, including models with no adapters, to get a qualitative picture of the effect on downstream performance. We use the same visual encoder (CLIP ‘RN50x16’) for all adapter ablations and evaluate the open-ended few-shot scores on the Visual Question Answering and Image Captioning tasks described in 4.1.1 and 4.1.2 respectively. The results are shown in Table 1.

Although there is no adapter configuration which clearly outperforms the rest, we observe three key points:

Applying adapters to the attention layer is key. Adapter configurations with no adapters on the attention layer underperform, particularly at few shot prompting.

Allocating more adapter parameters to the feed forward layer increases performance on knowledge-based tasks. The adapter variant with more parameters allocated to the feed forward adapter outperforms other variants on OKVQA and NoCaps, tasks which require outside knowledge and the ability to recognize uncommon object classes respectively. This reinforces preliminary research indicating that the Feed-Forward blocks play an important role in storing implicit knowledge in pretrained transformers [11].

Balancing attention and feed-forward parameter allocation aids scene understanding. The adapter variant where an equal number of parameters are allocated to the attention and the feed forward adapters excels at the GQA benchmark, a question answering benchmark built around scene graphs and designed to measure performance on skills such as spatial reasoning, comparisons, and object and attribute recognition.

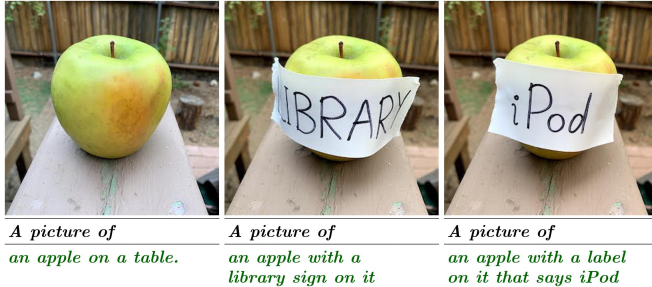


Figure 5. An example of an adversarial *typographic attack* which MAGMA appears robust to, unlike CLIP.

4.2.2 Visual Encoders

We run ablations using four different image encoders: NFResnet, CLIP-ViT-B/32, CLIP-RN50x4 and CLIP-RN50x16. All visual encoder ablations are trained using the adapter configuration with sequential adapters on the feed-forward block and a downsample factor of 4. The results are shown in Table 1.

Our findings are the following:

CLIP-RN50x16, on average, performs best at Visual Question Answering tasks. However, the difference between RN50x16 and RN50x4 is slight, with the smaller encoder performing better on VQA and OKVQA, while the larger encoder has a much higher GQA accuracy. We hypothesize that the increased resolution of the larger feature grid results in a more detailed scene understanding, while the smaller grid is better at condensing global visual information, which also shows in the Image Captioning scores, where CLIP-RN50x4 excels.

CLIP-ViT has the worst average score across question answering tasks. This reinforces the finding of [44], who find that the CLIP-ViT model struggles at tasks which require localization within an image.

Recall that the image prefix length varies between image encoders which may have a confounding effect on the results – further study is needed to disentangle the effects of sequence length and vision encoder.

4.3. Final Model

4.3.1 Performance

Based on our ablation studies, in particular the average Visual Question Answering scores, we opt to train a final MAGMA model using the CLIP-RN50x16 encoder and sequential adapters with a downsample factor of 8 applied to the feed-forward and attention layers. We train on the dataset detailed in Section 3.3, and observe that evaluation loss does not plateau after $\sim 3M$ samples as reported in *Frozen* [52], and so continue training, resulting in two model variants – $MAGMA_{base}$ trained for 15000 steps in

order to remain comparable to *Frozen*, and $MAGMA_{long}$, trained for around 7.6M samples.

Due to the inclusion of the training splits of downstream tasks in the pretraining dataset, the zero-shot performance of $MAGMA_{base}$ significantly exceeds the 4-shot performance of previously trained ablations - reinforcing the findings of [42, 56] that suggest the finetuning of pretrained LMs on structured task datasets substantially boosts zero-shot performance. We also found that the accuracy of $MAGMA_{base}$ no longer improves with an increasing number of shots, and so report no more than 0-shot in Table 1.

While the scores of $MAGMA_{long}$ already surpass the VQA-finetuned variants reported in *Frozen* [52], we find that we can further increase the single-task performance on the training sets of each benchmark described in Section 4.1. After finetuning, MAGMA achieves competitive scores across all benchmarks, setting a new state of the art accuracy on OKVQA, as well as attaining strong scores on the NoCaps benchmark - to our knowledge, being surpassed only by *SimVLM* and *VinVL* [60], see Table 2.

Aside from our quantitative experiments, we also include several qualitative results, which highlight capabilities of the model we feel are not sufficiently reflected by the evaluations in Table 1. Notably, MAGMA appears to be less easily fooled by the adversarial *typographic attacks* to which CLIP is susceptible [16], see Figure 5. Additionally, MAGMA shows impressive OCR capabilities even without supervised finetuning, see Figure 4, which warrants further quantitative evaluation. Interestingly, if a word or phrase is truncated, MAGMA can often impute the missing text. We also include an example of a multi-step *factored cognition* prompt [32], see Figure 6, where a challenging task is broken down into atomic steps. We suspect that task decomposition may enable MAGMA to perform complex tasks that it would otherwise be unable to solve.

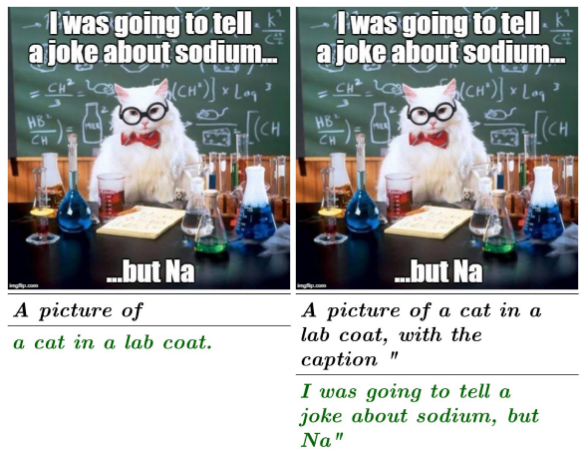


Figure 6. An example of a *multi-step prompting* procedure. Using the output of the model (left) again as the input (right), the generation procedure is broken down into atomic steps.

Table 1. Performance evaluation on downstream tasks.
 Open-ended few-shot evaluation on VQA-val, OKVQA-val, GQA-testdev and VizWiz-val.
 Captioning evaluation on NoCaps-val and CoCo-val.

Type: (s)caled or (p)arallel. λ : 1 or (t)rained. **Attn, FF:** Downsample factor of the bottleneck in the resp. position. – means not applied.

Adapter ablations					n -shot-VQA				n -shot-OKVQA				n -shot-GQA				n -shot-VizWiz				Avg.	
Type	λ	Attn	FF	params	0	1	2	4	0	1	2	4	0	1	2	4	0	1	2	4		
–	–	–	–	0.1	36.4	41.5	41.7	41.8	12.5	16.2	16.0	16.5	12.6	20.8	23.6	26.9	2.9	5.3	5.5	6.7	20.4	
s	1	–	2	2	34.7	40.1	42.2	43.2	12.4	16.9	18.6	21.5	8.2	14.1	19.2	24.6	5.3	7.4	7.8	9.7	20.4	
s	1	–	4	1	32.7	40.2	42.5	43.8	11.7	16.3	19.1	21.2	6.8	15.6	22.1	27.7	4.2	6.7	6.9	8.6	20.0	
s	1	8	8	1	36.6	41.7	43.8	45.2	13.9	17.1	20.0	22.5	14.3	20.7	24.9	28.4	5.6	8.5	8.6	9.8	22.6	
s	1	12	6	1	36.9	41.2	43.6	44.7	13.9	19.4	21.6	23.2	12.8	18.8	22.5	25.8	5.3	9.6	9.8	10.6	22.5	
p	1	–	4	1	36.5	41.7	43.1	43.8	14.5	18.4	20.3	21.8	11.2	16.3	19.9	23.2	4.6	8.4	8.4	9.2	21.3	
p	t	8	8	1	34.9	42.2	44.1	45.4	12.9	17.7	21.4	23.4	8.8	15.6	20.2	24.5	4.3	7.9	8.5	9.9	21.4	
Encoder ablations																						
					32.0	37.0	39.0	39.7	9.8	15.8	18.9	20.8	9.1	20.2	27.1	28.7	2.8	5.6	6.5	8.2	20.1	
					32.8	33.9	36.7	37.7	10.5	9.2	12.4	14.2	8.4	14.9	22.2	25.7	2.7	5.1	5.2	7.7	17.5	
					35.2	40.0	42.6	44.2	12.6	17.7	19.0	21.8	10.5	13.0	16.1	20.5	5.0	6.2	6.6	8.3	20.0	
					32.7	40.2	42.5	43.8	11.7	16.3	19.1	21.2	6.8	15.6	22.1	27.7	4.2	6.7	6.9	8.6	20.4	
MAGMA pretrained																						
					MAGMA _{froz}	28.6	36.7	37.9	38.1	6.2	15.1	16.2	15.8	8.7	23.5	27.0	27.5	1.7	5.4	6.2	8.0	18.9
					MAGMA _{base}	60.0	–	–	–	37.6	–	–	–	47.4	–	–	–	15.9	–	–	–	40.3
					MAGMA _{long}	61.5	–	–	–	40.3	–	–	–	49.6	–	–	–	16.7	–	–	–	42.0
Adapter ablations					NoCaps - CIDEr				NoCaps - B@4				CoCo - CIDEr				CoCo - B@4					
Type	λ	Attn	FF	params	In	Out	Near	All	In	Out	Near	All										
–	–	–	–	0.1	45.1	53.7	43.3	45.7	9.9	5.8	7.9	7.8	36.7				10.3					
s	1	–	2	2	37.7	55.5	40.6	43.2	6.2	6.1	6.5	6.4	33.4				9.4					
s	1	–	4	1	39.3	56.2	44.0	45.8	6.3	6.7	7.7	7.3	39.6				11.2					
s	1	8	8	1	38.2	49.5	40.9	42.2	6.4	4.9	6.7	6.3	37.1				10.6					
s	1	12	6	1	51.9	64.8	54.6	56.2	11.4	8.4	11.3	10.8	46.3				13.9					
p	1	–	4	1	37.5	38.1	35.9	36.0	7.2	5.1	6.7	6.4	36.3				10.8					
p	t	8	8	1	40.6	58.3	45.0	47.1	8.0	6.6	7.9	7.7	39.5				11.2					
Encoder ablations																						
					22.5	16.2	22.0	20.9	5.0	1.6	5.3	4.5	22.4				8.2					
					33.2	44.2	35.3	36.8	5.9	5.2	5.8	5.7	27.2				7.7					
					47.7	43.6	48.1	50.2	9.3	6.7	9.2	8.7	41.9				13.1					
					39.3	56.2	44.0	45.8	6.3	6.7	7.7	7.3	39.6				11.2					
MAGMA pretrained																						
					MAGMA _{base}	55.8	56.5	49.9	52.1	11.1	6.1	10.3	9.5	51.1				15.8				
					MAGMA _{long}	58.1	62.0	56.9	58.1	13.3	8.5	13.2	12.3	57.0				17.6				

Table 2. MAGMA finetuned performance. **C:** CIDEr, **B:** B@4, NoCaps-all score. SOTA models and scores to the best of our knowledge.

	VQA	OKVQA	GQA	VizWiz	SNLI-VE	NoCaps		Coco	
						C	B	C	B
MAGMA	68.0	49.2	54.5	35.4	79.0	93.6	27.8	91.2	31.4
SOTA	75.5	48.0	72.1	54.7	86.3	112.2	33.1	143.3	41.7
SOTA model	<i>SimVLM</i> [55]	<i>PICa</i> [58]	<i>CFR</i> [33]	<i>Pythia</i> [46]	<i>SimVLM</i>	<i>SimVLM</i>	<i>VIVO</i> [22]	<i>SimVLM</i>	<i>OSCAR</i> [29]

4.3.2 Limitations

Although the performance of MAGMA is impressive, we note some current limitations with the model and autoregressive VL models in general. Firstly, as we observed in

the Image Captioning tasks, LMs can be sensitive to input – performance is heavily dependent on the prompt format.

Secondly, although the model can perform in-context learning with multiple examples in its context window, it struggles to reason over multiple images, as it was only pre-

trained on single image-caption pairs.

Finally, MAGMA shows similar capabilities to large LMs like GPT3, about which there are ongoing ethical concerns regarding their reproduction of biases from the training data, as well as concerns relating to how to effectively align their outputs to human goals. As such, further research into the reproduction of visual biases, and the guiding of model outputs is needed.

5. Conclusion

In this work, we propose a simple framework for the Multimodal Augmentation of Generative Models through Adapter-based Finetuning – demonstrating that it is possible to transform multiple unimodal models into a powerful multimodal VL model whilst keeping the weights of the language component frozen. Our model, MAGMA, trained using adapter layers and a simple next token prediction objective, can perform competitively with state of the art VL models on a wide range of benchmarks, excelling at tasks requiring external knowledge and the recognition of uncommon object classes.

We hope our results will act as a starting point for further research into augmenting pretrained language models with additional modalities.

References

- [1] Harsh Agrawal, Karan Desai, Yufei Wang, Xinlei Chen, Rishabh Jain, Mark Johnson, Dhruv Batra, Devi Parikh, Stefan Lee, and Peter Anderson. nocaps: novel object captioning at scale. *2019 IEEE/CVF International Conference on Computer Vision (ICCV)*, Oct 2019. 6
- [2] Stanislaw Antol, Aishwarya Agrawal, Jiasen Lu, Margaret Mitchell, Dhruv Batra, C. Lawrence Zitnick, and Devi Parikh. VQA: Visual Question Answering. In *International Conference on Computer Vision (ICCV)*, 2015. 5, 6
- [3] Sid Black, Leo Gao, Phil Wang, Connor Leahy, and Stella Biderman. GPT-Neo: Large Scale Autoregressive Language Modeling with Mesh-Tensorflow, Mar. 2021. If you use this software, please cite it using these metadata. 2
- [4] Samuel R. Bowman, Gabor Angeli, Christopher Potts, and Christopher D. Manning. A large annotated corpus for learning natural language inference. *CoRR*, abs/1508.05326, 2015. 6
- [5] Andrew Brock, Soham De, Samuel L. Smith, and Karen Simonyan. High-performance large-scale image recognition without normalization. *CoRR*, abs/2102.06171, 2021. 2
- [6] Tom B. Brown, Benjamin Mann, Nick Ryder, Melanie Subbiah, Jared Kaplan, Prafulla Dhariwal, Arvind Neelakantan, Pranav Shyam, Girish Sastry, Amanda Askell, Sandhini Agarwal, Ariel Herbert-Voss, Gretchen Krueger, Tom Henighan, Rewon Child, Aditya Ramesh, Daniel M. Ziegler, Jeffrey Wu, Clemens Winter, Christopher Hesse, Mark Chen, Eric Sigler, Mateusz Litwin, Scott Gray, Benjamin Chess, Jack Clark, Christopher Berner, Sam McCandlish, Alec Radford, Ilya Sutskever, and Dario Amodei. Language models are few-shot learners, 2020. 1, 2, 5
- [7] Soravit Changpinyo, Piyush Sharma, Nan Ding, and Radu Soricut. Conceptual 12m: Pushing web-scale image-text pre-training to recognize long-tail visual concepts. *CoRR*, abs/2102.08981, 2021. 2, 5
- [8] Soravit Changpinyo, Piyush Sharma, Nan Ding, and Radu Soricut. Conceptual 12m: Pushing web-scale image-text pre-training to recognize long-tail visual concepts. *CoRR*, abs/2102.08981, 2021. 5
- [9] Xinlei Chen, Hao Fang, Tsung-Yi Lin, Ramakrishna Vedantam, Saurabh Gupta, Piotr Dollár, and C. Lawrence Zitnick. Microsoft COCO captions: Data collection and evaluation server. *CoRR*, abs/1504.00325, 2015. 5, 6
- [10] Yen-Chun Chen, Linjie Li, Licheng Yu, Ahmed El Kholy, Faisal Ahmed, Zhe Gan, Yu Cheng, and Jingjing Liu. Uniter: Universal image-text representation learning, 2019. 2
- [11] Damai Dai, Li Dong, Yaru Hao, Zhifang Sui, and Furu Wei. Knowledge neurons in pretrained transformers. *CoRR*, abs/2104.08696, 2021. 6
- [12] Jacob Devlin, Ming-Wei Chang, Kenton Lee, and Kristina Toutanova. Bert: Pre-training of deep bidirectional transformers for language understanding, 2019. 1
- [13] Alexey Dosovitskiy, Lucas Beyer, Alexander Kolesnikov, Dirk Weissenborn, Xiaohua Zhai, Thomas Unterthiner, Mostafa Dehghani, Matthias Minderer, Georg Heigold, Sylvain Gelly, et al. An image is worth 16x16 words: Transformers for image recognition at scale. *arXiv preprint arXiv:2010.11929*, 2020. 2
- [14] Patrick Esser, Robin Rombach, and Bjorn Ommer. Taming transformers for high-resolution image synthesis. In *Proceedings of the IEEE/CVF Conference on Computer Vision and Pattern Recognition*, pages 12873–12883, 2021. 3
- [15] Leo Gao, Stella Biderman, Sid Black, Laurence Golding, Travis Hoppe, Charles Foster, Jason Phang, Horace He, Anish Thite, Noa Nabeshima, Shawn Presser, and Connor Leahy. The pile: An 800gb dataset of diverse text for language modeling. *CoRR*, abs/2101.00027, 2021. 5
- [16] Gabriel Goh, Nick Cammarata †, Chelsea Voss †, Shan Carter, Michael Petrov, Ludwig Schubert, Alec Radford, and Chris Olah. Multimodal neurons in artificial neural networks. *Distill*, 2021. <https://distill.pub/2021/multimodal-neurons>. 7
- [17] Danna Gurari, Qing Li, Abigale J. Stangl, Anhong Guo, Chi Lin, Kristen Grauman, Jiebo Luo, and Jeffrey P. Bigham. Vizwiz grand challenge: Answering visual questions from blind people. *CoRR*, abs/1802.08218, 2018. 5
- [18] Junxian He, Chunting Zhou, Xuezhe Ma, Taylor Berg-Kirkpatrick, and Graham Neubig. Towards a unified view of parameter-efficient transfer learning, 2021. 3, 4, 6
- [19] Kaiming He, Xiangyu Zhang, Shaoqing Ren, and Jian Sun. Deep residual learning for image recognition. *CoRR*, abs/1512.03385, 2015. 2
- [20] Neil Houlsby, Andrei Giurgiu, Stanislaw Jastrzebski, Bruna Morrone, Quentin de Laroussilhe, Andrea Gesmundo, Mona Attariyan, and Sylvain Gelly. Parameter-efficient transfer learning for nlp, 2019. 3, 4

- [21] Edward J. Hu, Yelong Shen, Phillip Wallis, Zeyuan Allen-Zhu, Yuanzhi Li, Shean Wang, and Weizhu Chen. Lora: Low-rank adaptation of large language models. *CoRR*, abs/2106.09685, 2021. 3
- [22] Xiaowei Hu, Xi Yin, Kevin Lin, Lijuan Wang, Lei Zhang, Jianfeng Gao, and Zicheng Liu. VIVO: surpassing human performance in novel object captioning with visual vocabulary pre-training. *CoRR*, abs/2009.13682, 2020. 8
- [23] Drew A. Hudson and Christopher D. Manning. GQA: a new dataset for compositional question answering over real-world images. *CoRR*, abs/1902.09506, 2019. 5
- [24] Chao Jia, Yinfei Yang, Ye Xia, Yi-Ting Chen, Zarana Parekh, Hieu Pham, Quoc V. Le, Yunhsuan Sung, Zhen Li, and Tom Duerig. Scaling up visual and vision-language representation learning with noisy text supervision, 2021. 3
- [25] Douwe Kiela, Hamed Firooz, Aravind Mohan, Vedanuj Goswami, Amanpreet Singh, Pratik Ringshia, and Davide Testuggine. The hateful memes challenge: Detecting hate speech in multimodal memes. *CoRR*, abs/2005.04790, 2020. 5
- [26] Ranjay Krishna, Yuke Zhu, Oliver Groth, Justin Johnson, Kenji Hata, Joshua Kravitz, Stephanie Chen, Yannis Kalantidis, Li-Jia Li, David A Shamma, Michael Bernstein, and Li Fei-Fei. Visual genome: Connecting language and vision using crowdsourced dense image annotations. 2016. 5
- [27] Brian Lester, Rami Al-Rfou, and Noah Constant. The power of scale for parameter-efficient prompt tuning, 2021. 3
- [28] Liunian Harold Li, Mark Yatskar, Da Yin, Cho-Jui Hsieh, and Kai-Wei Chang. Visualbert: A simple and performant baseline for vision and language, 2019. 2
- [29] Xiujun Li, Xi Yin, Chunyuan Li, Pengchuan Zhang, Xiaowei Hu, Lei Zhang, Lijuan Wang, Houdong Hu, Li Dong, Furu Wei, Yejin Choi, and Jianfeng Gao. Oscar: Object-semantics aligned pre-training for vision-language tasks, 2020. 2, 8
- [30] Xiang Lisa Li and Percy Liang. Prefix-tuning: Optimizing continuous prompts for generation, 2021. 3
- [31] Kenneth Marino, Mohammad Rastegari, Ali Farhadi, and Roozbeh Mottaghi. Ok-vqa: A visual question answering benchmark requiring external knowledge. In *Conference on Computer Vision and Pattern Recognition (CVPR)*, 2019. 5
- [32] Swaroop Mishra, Daniel Khashabi, Chitta Baral, Yejin Choi, and Hannaneh Hajishirzi. Reframing instructional prompts to gptk’s language, 2021. 7
- [33] Binh X. Nguyen, Tuong Do, Huy Tran, Erman Tjiputra, Quang D. Tran, and Anh Nguyen. Coarse-to-fine reasoning for visual question answering, 2021. 8
- [34] Jonas Pfeiffer, Andreas Rücklé, Clifton Poth, Aishwarya Kamath, Ivan Vulic, Sebastian Ruder, Kyunghyun Cho, and Iryna Gurevych. Adapterhub: A framework for adapting transformers. *CoRR*, abs/2007.07779, 2020. 3
- [35] Jordi Pont-Tuset, Jasper Uijlings, Soravit Changpinyo, Radu Soricut, and Vittorio Ferrari. Connecting vision and language with localized narratives. In *ECCV*, 2020. 5
- [36] Guanghui Qin and Jason Eisner. Learning how to ask: Querying LMs with mixtures of soft prompts. In *Proceedings of the 2021 Conference of the North American Chapter of the Association for Computational Linguistics: Human Language Technologies (NAACL-HLT)*, pages 5203–5212, Online, June 2021. Best Short Paper Award. 3
- [37] Alec Radford, Jong Wook Kim, Chris Hallacy, Aditya Ramesh, Gabriel Goh, Sandhini Agarwal, Girish Sastry, Amanda Askell, Pamela Mishkin, Jack Clark, Gretchen Krueger, and Ilya Sutskever. Learning transferable visual models from natural language supervision, 2021. 2, 3, 5
- [38] Alec Radford, Karthik Narasimhan, Tim Salimans, and Ilya Sutskever. Improving language understanding by generative pre-training. 2018. 1, 4
- [39] Alec Radford, Jeffrey Wu, Rewon Child, David Luan, Dario Amodei, and Ilya Sutskever. Language models are unsupervised multitask learners. *OpenAI blog*, 1(8):9, 2019. 1
- [40] Samyam Rajbhandari, Jeff Rasley, Olatunji Ruwase, and Yuxiong He. Zero: Memory optimization towards training A trillion parameter models. *CoRR*, abs/1910.02054, 2019. 5
- [41] Shaoqing Ren, Kaiming He, Ross Girshick, and Jian Sun. Faster r-cnn: Towards real-time object detection with region proposal networks. *Advances in neural information processing systems*, 28:91–99, 2015. 1, 3
- [42] Victor Sanh, Albert Webson, Colin Raffel, Stephen H. Bach, Lintang Sutawika, Zaid Alyafeai, Antoine Chaffin, Arnaud Stiegler, Teven Le Scao, Arun Raja, Manan Dey, M Saiful Bari, Canwen Xu, Urmish Thakker, Shanya Sharma Sharma, Eliza Szczechla, Taewoon Kim, Gunjan Chhablani, Nihal Nayak, Debajyoti Datta, Jonathan Chang, Mike Tian-Jian Jiang, Han Wang, Matteo Manica, Sheng Shen, Zheng Xin Yong, Harshit Pandey, Rachel Bawden, Thomas Wang, Trishala Neeraj, Jos Rozen, Abheesht Sharma, Andrea Santilli, Thibault Fevry, Jason Alan Fries, Ryan Teehan, Stella Biderman, Leo Gao, Tali Bers, Thomas Wolf, and Alexander M. Rush. Multitask prompted training enables zero-shot task generalization, 2021. 5, 7
- [43] Christoph Schuhmann, Richard Vencu, Romain Beaumont, Robert Kaczmarczyk, Clayton Mullis, Aarush Katta, Theo Coombes, Jenia Jitsev, and Aran Komatsuzaki. Laion-400m: Open dataset of clip-filtered 400 million image-text pairs, 2021. 5
- [44] Sheng Shen, Liunian Harold Li, Hao Tan, Mohit Bansal, Anna Rohrbach, Kai-Wei Chang, Zhewei Yao, and Kurt Keutzer. How much can clip benefit vision-and-language tasks?, 2021. 3, 7
- [45] Taylor Shin, Yasaman Razeghi, Robert L. Logan IV au2, Eric Wallace, and Sameer Singh. Autoprompt: Eliciting knowledge from language models with automatically generated prompts, 2020. 3
- [46] Amanpreet Singh, Vivek Natarajan, Meet Shah, Yu Jiang, Xinlei Chen, Dhruv Batra, Devi Parikh, and Marcus Rohrbach. Towards VQA models that can read. *CoRR*, abs/1904.08920, 2019. 8
- [47] Michael Sollami and Aashish Jain. Multimodal conditionality for natural language generation, 2021. 1
- [48] Krishna Srinivasan, Karthik Raman, Jiecao Chen, Michael Bendersky, and Marc Najork. WIT: wikipedia-based image text dataset for multimodal multilingual machine learning. *CoRR*, abs/2103.01913, 2021. 5

- [49] Jianlin Su, Yu Lu, Shengfeng Pan, Bo Wen, and Yunfeng Liu. Roformer: Enhanced transformer with rotary position embedding. *CoRR*, abs/2104.09864, 2021. 4
- [50] Weijie Su, Xizhou Zhu, Yue Cao, Bin Li, Lewei Lu, Furu Wei, and Jifeng Dai. Vi-bert: Pre-training of generic visual-linguistic representations, 2020. 2
- [51] Hao Tan and Mohit Bansal. Lxmert: Learning cross-modality encoder representations from transformers, 2019. 2
- [52] Maria Tsimpoukelli, Jacob Menick, Serkan Cabi, S. M. Ali Eslami, Oriol Vinyals, and Felix Hill. Multimodal few-shot learning with frozen language models. *CoRR*, abs/2106.13884, 2021. 1, 2, 3, 4, 6, 7
- [53] Ashish Vaswani, Noam Shazeer, Niki Parmar, Jakob Uszkoreit, Llion Jones, Aidan N Gomez, Łukasz Kaiser, and Illia Polosukhin. Attention is all you need. In *Advances in neural information processing systems*, pages 5998–6008, 2017. 1
- [54] Ben Wang and Aran Komatsuzaki. GPT-J-6B: A 6 Billion Parameter Autoregressive Language Model. <https://github.com/kingoflolz/mesh-transformer-jax>, May 2021. 2, 4
- [55] Zirui Wang, Jiahui Yu, Adams Wei Yu, Zihang Dai, Yulia Tsvetkov, and Yuan Cao. Simvln: Simple visual language model pretraining with weak supervision, 2021. 1, 2, 8
- [56] Jason Wei, Maarten Bosma, Vincent Y. Zhao, Kelvin Guu, Adams Wei Yu, Brian Lester, Nan Du, Andrew M. Dai, and Quoc V. Le. Finetuned language models are zero-shot learners, 2021. 5, 7
- [57] Ning Xie, Farley Lai, Derek Doran, and Asim Kadav. Visual entailment task for visually-grounded language learning. *CoRR*, abs/1811.10582, 2018. 6
- [58] Zhengyuan Yang, Zhe Gan, Jianfeng Wang, Xiaowei Hu, Yumao Lu, Zicheng Liu, and Lijuan Wang. An empirical study of gpt-3 for few-shot knowledge-based vqa, 2021. 8
- [59] Wei Zeng, Xiaozhe Ren, Teng Su, Hui Wang, Yi Liao, Zhiwei Wang, Xin Jiang, ZhenZhang Yang, Kaisheng Wang, Xiaoda Zhang, Chen Li, Ziyang Gong, Yifan Yao, Xinjing Huang, Jun Wang, Jianfeng Yu, Qi Guo, Yue Yu, Yan Zhang, Jin Wang, Hengtao Tao, Dasen Yan, Zexuan Yi, Fang Peng, Fangqing Jiang, Han Zhang, Lingfeng Deng, Yehong Zhang, Zhe Lin, Chao Zhang, Shaojie Zhang, Mingyue Guo, Shanzhi Gu, Gaojun Fan, Yaowei Wang, Xuefeng Jin, Qun Liu, and Yonghong Tian. Pangu- α : Large-scale autoregressive pretrained chinese language models with auto-parallel computation, 2021. 2
- [60] Pengchuan Zhang, Xiujun Li, Xiaowei Hu, Jianwei Yang, Lei Zhang, Lijuan Wang, Yejin Choi, and Jianfeng Gao. Vinvl: Revisiting visual representations in vision-language models. 2021. 2, 5, 7